

# Utilizing laser interference lithography to fabricate hierarchical optical active nanostructures inspired by the blue *Morpho* butterfly

Radwanul H. Siddique<sup>a</sup>, Abrar Faisal<sup>a</sup>, Ruben Hünig<sup>b</sup>, Carolin Bartels<sup>c</sup>, Irene Wacker<sup>c</sup>, Uli Lemmer<sup>b</sup> and Hendrik Hölscher<sup>a</sup>

<sup>a</sup>Institute for Microstructure Technology (IMT), Karlsruhe Institute of Technology (KIT), 76344 Eggenstein-Leopoldshafen, Germany;

<sup>b</sup>Light Technology Institute (LTI), Karlsruhe Institute of Technology (KIT), 76131 Karlsruhe, Germany;

<sup>c</sup>Center for Advanced Materials (CAM), University of Heidelberg, 69120 Heidelberg, Germany

## ABSTRACT

The famous non-iridescent blue of the *Morpho* butterfly is caused by a ‘Christmas tree’ like nanostructure which is a challenge for common fabrication techniques. Here, we introduce a method to fabricate this complex morphology utilizing dual beam interference lithography. We add a reflective coating below the photoresist to create a second interference pattern in vertical direction by exploiting the back reflection from the substrate. This vertical pattern exposes the lamella structure into the photosensitive polymer while the horizontal interference pattern determines the distance of the ridges. The photosensitive polymer is chosen accordingly to create the ‘Christmas tree’ like tapered shape. The resulting artificial *Morpho* replica shows brilliant non-iridescent blue up to an incident angle of 40°. Its optical properties are close to the original *Morpho* structure because the refractive index of the polymer is close to that of chitin. Moreover, the biomimetic surface is water repellent with a contact angle of 110°.

**Keywords:** *Morpho* butterfly nanostructures, Biomimetics, Bio-inspired optics/photonics, Laser interference lithography

## 1. INTRODUCTION

The *Morpho* butterfly originating from South America is a famous example for structural color in nature. The blue metallic shimmering of its scales (Fig. 1) attracted the attention of researchers for decades.<sup>1–4</sup> There have been numerous theoretical and numerical studies on how light interacts with ‘Christmas tree’ like structure (see Fig. 1) which forms an alternating stack of air and chitin.<sup>5–11</sup> Most of the studies found that multilayer interference caused by the lamellae is the main reason of the blue omni-directional reflection. Employing this concept, Saito *et al.*<sup>12</sup> and Chung *et al.*<sup>13</sup> used multilayer deposition of TiO<sub>2</sub>/SiO<sub>2</sub> on an irregular support to achieve the wide angular reflectance of the blue color. However, the exact replication of the complex ‘Christmas tree’ like nanostructure, specially on large area is needed to utilize *Morpho* structures for advanced applications like self-cleaning optical coatings,<sup>14</sup> selective gas/vapor sensors,<sup>15</sup> thermal imaging sensors,<sup>16</sup> and efficient solar cells.<sup>17</sup> Watanabe *et al.* fabricated replica of *Morpho* butterfly structures by focused-ion-beam chemical-vapor-deposition (FIB-CVD). This serial approach, however, is not a solution for large scale applications. Recently, Aryal *et al.*<sup>18</sup> introduced a promising approach for the large scale fabrication based on chemical vapor deposition, wet chemical etching, and subsequent nanoimprint of three dimensional butterfly structures. Nonetheless, the refractive indexes of the used materials (Si<sub>3</sub>N<sub>4</sub>, SiO<sub>2</sub>, and Si substrate;  $n = 1.5–3.6$ ) vary and did not match that of Chitin (1.56) and nanoimprinting the high undercut of the structure with polymers is challenging. Therefore, it remains difficult to obtain the famous omnidirectional blue reflection of the *Morpho* butterfly on large areas by a direct replication of the ‘Christmas tree’ like nanostructure.

---

Further author information: (Send correspondence to Radwanul H. Siddique  
Radwanul H. Siddique: E-mail: radwanul.siddique@kit.edu)

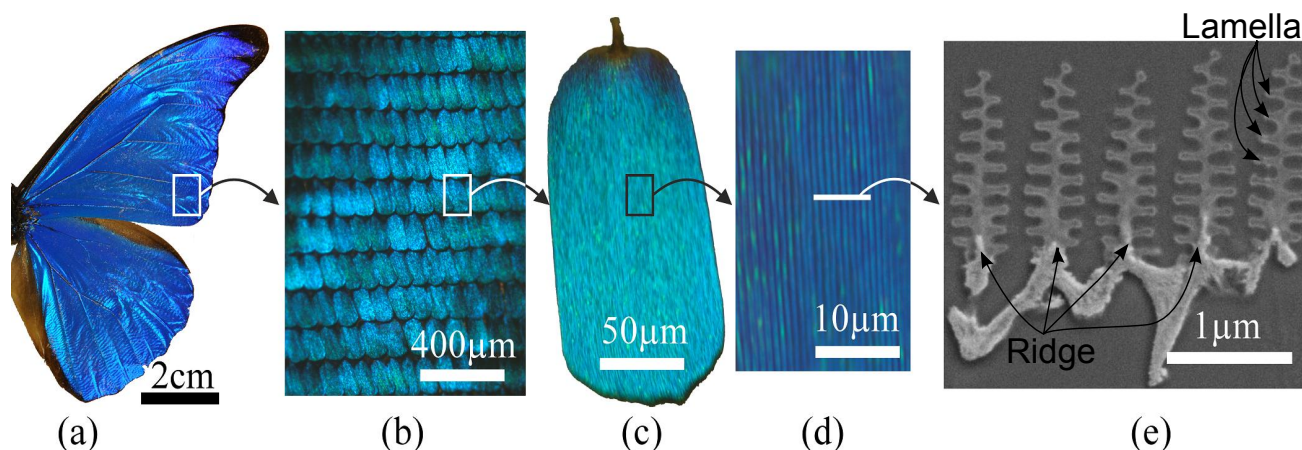


Figure 1. Zooming into the structural patterns of the *Morpho rhetenor* butterfly: from the whole wing into the 'Christmas tree' like nanostructure inside the scales. a) Photo of a *Morpho rhetenor* butterfly wing. b) Photo of the blue scales which are arranged like shingles on a roof. c) A single scale has a typical width and length of  $80\ \mu\text{m}$  and  $200\ \mu\text{m}$ , respectively. d) The optical microscopy image shows the quasi-periodic structure of the ridges. e) The SEM image of the cross-section of the ridges reveals the 'Christmas tree' like nanostructure which forms a multilayer stack of air and chitin.

Here, we introduce a technique to fabricate the Christmas tree like morphology utilizing dual beam laser interference lithography (LIL)<sup>19–23</sup> on a glass substrate. Dual beam LIL is widely used for the fabrication of one dimensional periodic patterns on the micrometer or sub-micrometer scale. In difference to this conventional approach, we use a reflective coating below the substrate to create an additional vertical interference. These vertical standing wave patterns are an unwanted artifact in classical LIL<sup>23</sup> but in our case they help to write the lamella structure into the resist. The conventional horizontal grating structure forms the ridges. Depending on the period of the vertical standing wave and the photoresist, the thickness of the lamella and gap of air between them can be adjusted. A low contrast photoresist is used to obtain the triangular tapered shape of the 'Christmas tree' like structure. The resulting *Morpho* structures show brilliant blue non-iridescence up to an incident angle of  $40^\circ$ . Moreover, due to its hierarchical structure the surface is strongly water repellent. This feature is important for the design of self-cleaning optical coatings.

## 2. FABRICATION

To fabricate the 'Christmas tree' like nanostructure inspired by the blue *Morpho* butterfly we exploited classical dual beam laser interference lithography (LIL).<sup>20,23</sup> The classical steps of laser interference lithography are summarized in Fig. 2a). First, a photoresist is spin-coated onto a clean glass substrate. After that the photoresist is exposed by a dual laser beam with an experimental setup schematically depicted in Fig. 2b). In order to satisfy the high coherence requirement of LIL, two incident laser beams are split from the same laser source, and travel the same optical length when reaching the sample. Our experimental setup uses a frequency-quadrupled Nd:YVO4 solid state laser with an operation wavelength of 266 nm and a maximum output of 200 mW (Type 1 CW 266- 100, Model FQCW 266- 100, CryLas GmbH, Berlin, Germany). In order to expose large sample areas of  $25\ \text{mm} \times 25\ \text{mm}$ , the lithography setup employs a dual beam Mach-Zehnder interferometer architecture. The emitted laser beam is split by a 50:50 beam splitter. Then, the two split laser beams are deflected towards two corresponding lenses by planar aluminum mirrors, which can be rotated by high-resolution electrical rotation stages to select the irradiation angle  $\theta$ . The lenses expand the beams, to increase the exposure area. To improve the beam quality, one pinhole is placed after each lens. The pinholes spatially filter out the high-frequency distortions, caused by, e.g., stray centers found on the optical components or suspended in the surrounding air, and by system inherent optical errors.<sup>23</sup> If not filtered out, these deviations might cause inhomogeneities of the Gaussian beam profile, leading to undesired low-quality exposure results. As the experiment requires equal intensity of the two expanded beams, a rotatable quartz plate is placed in one of the optical paths, to fine-tune the transmitted power. The reflected part of the beam is guided to a photodiode for power monitoring. Finally, the two expanded beams interfere on the sample surface. For beam-blanking a mechanical shutter is used. The

exposure dosage into the photoresist is controlled by a Labview program on a PC, which records the real-time power of the laser via the photodiode and operates the mechanical shutter. The setup is calibrated by referencing the photodiode signal to the laser power at the sample position prior to the exposure by using a laser power analyzer. The photodiode is then read out during the exposure and allows for precise control of the shutter opening time to establish the desired dosage.

Figure 2c) shows the resulting triangular grating structure obtained with this setup. Depending on the photoresist – its sensitivity to exposure wavelength and its selectivity towards the developer – either rectangular, sinusoidal or triangular grating profiles can be achieved. In order to realize a triangular geometry, a photoresist with low contrast and sensitivity is required. We chose AZ photoresist (AZ 1505, Microchemicals GmbH, Ulm, Germany) which has low sensitivity in the deep UV regime (266 nm). In this way we obtain the triangular or tapered shape like structure of the ‘Christmas tree’ of the *Morpho* butterfly. Fused silica (25 mm × 25 mm × 1 mm) is used as a substrate and sputtered with a thin reflective optical coating ( $R > 99.5\%$  at wavelengths of 250–280 nm) by LASEROPTK GmbH, Garbsen, Germany. The average reflectance of the coating is well below 5% in the visible range. Photoresist is spin-coated on the substrate with a speed of 3000 rpm, an acceleration of 1500 rpm/s for 60 seconds to achieve 500 nm thickness. The prebake was performed on a hotplate at 95°C for 3 minutes. The parameters were chosen adequately to realize a low contrast system, allowing for direct transfer of the interference pattern into the photoresist. The exposure dosage was 250 mJ/cm<sup>2</sup>. The KOH-based AZ 400K (1:4 diluted) developer (Microchemicals GmbH, Ulm, Germany) is used to develop the sample for 15 seconds due to its lower selectivity to achieve the triangular shape.

Three dimensional structures can be created by LIL utilizing an interference pattern of four or more laser beams. The exact shape is controlled by the relative phase, intensity, polarization, and direction of the laser beams.<sup>21</sup> Here, we extended dual beam interference to produce the famous ‘Christmas tree’ like shape in a single step. To achieve that, we added a reflective surface below the photoresist to create an additional vertical secondary interference. It creates the multilayer structure of lamellae while the horizontal interference pattern structures the ridges. The fabrication steps are summarized in Fig. 3a). The fabrication process consists of three main steps: sample preparation, exposure and development.

The important factor to create the proper vertical standing wave pattern is the reflective thin film coating. Commonly used silicon substrates are reflective in the UV regime and create standing wave patterns from the back reflection. As silicon reflects  $\approx 60\%$  at lower angles, the modulation depth is lower.<sup>23</sup> Hence, this effect creates a small modulation in the resist.<sup>24</sup> Aluminium is the right choice for deep UV exposure as it reflects more than 90% at an exposure wavelength of 266 nm. However, in order to improve the optical properties of the final samples in the visible regime, we added a thin optical coating onto a glass substrate. It reflects almost 100% between 250–280 nm and is nearly transparent for other wavelengths. The SEM images in Fig. 3b) reveal the obtained lamellae structure forming the multilayer of photoresist and air. As expected the sample shows the blue reflection (Fig. 3c). There is a layer of residue left at the surface of unresolved resist due to the standing wave intensity-knot pattern in the positive photoresist.<sup>25</sup>

The horizontal period  $P_h$  of the structures in the  $x$ - $y$  plane is around  $1.8 \mu\text{m}$  which can be calculated by<sup>22</sup>

$$P_h = \frac{\lambda}{2n_s \sin \theta} \quad (1)$$

Here,  $\lambda$  is the wavelength of two incident laser beams, i.e., 266 nm,  $n_s$  stands for the refractive index of the surrounding medium, i.e., air and  $\theta$  is the angle between the surface normal and the incident laser beam. In the presented case,  $\theta$  was set to  $4.2^\circ$  to get a theoretical period of  $1.815 \mu\text{m}$ .

The vertical period  $P_v$  can be calculated with the equation<sup>23</sup>

$$P_v = \frac{\lambda}{2n_m \cos(\sin^{-1}(\sin \theta / n_m))} \quad (2)$$

Where,  $n_m$  is the refractive index of the polymer. It is 1.65 at 435 nm<sup>26</sup> and therefore, the theoretical vertical period is 80.7 nm. The experimental value of the vertical period is  $(83 \pm 2)$  nm fitting nicely to the theoretical value.

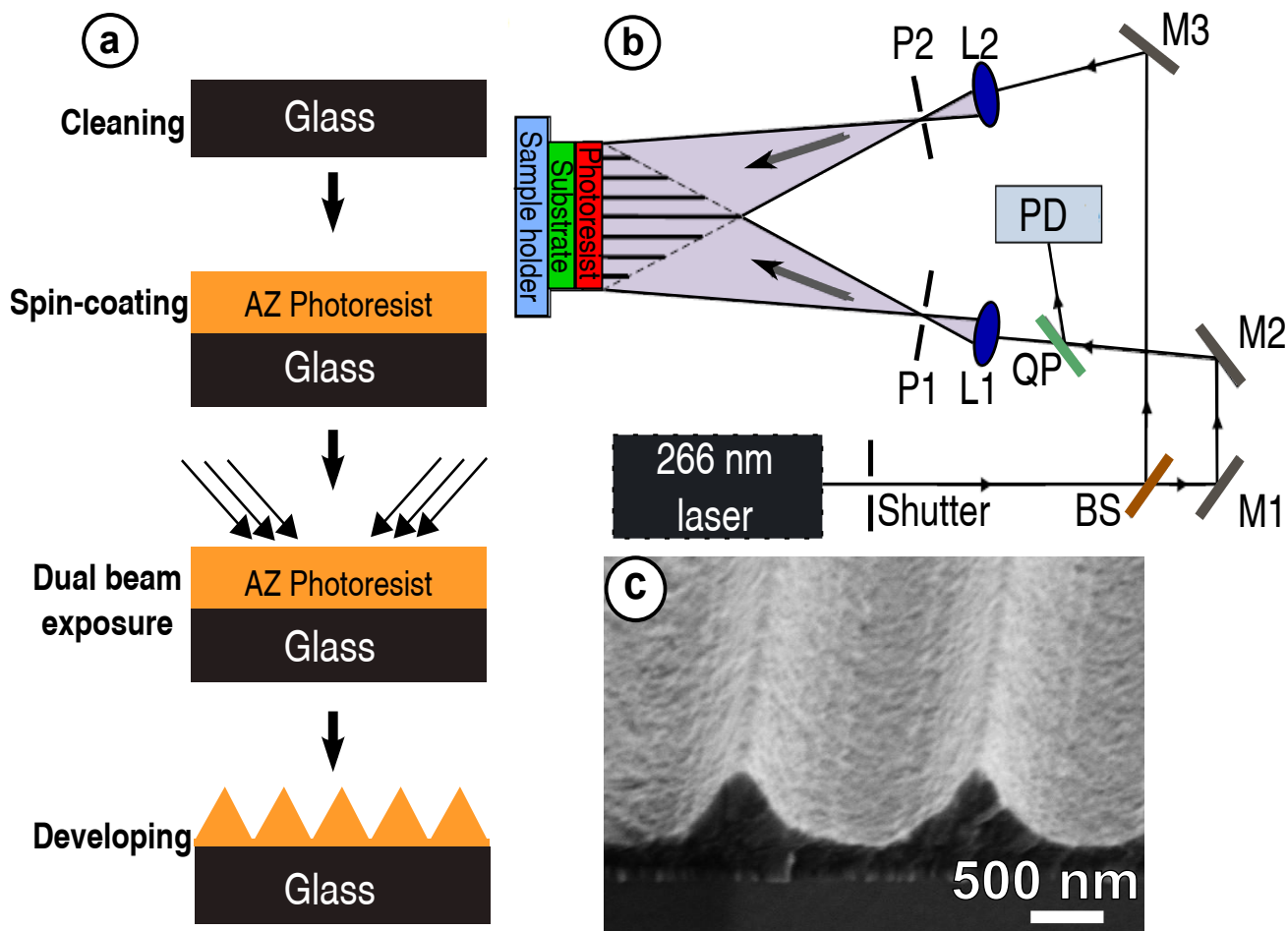


Figure 2. **a)** Flow diagram of the fabrication process of horizontal structures by dual beam laser interference lithography. A photoresist is spin-coated on a clean glass substrate and exposed by two interfering laser beams. After development of the photoresist, the interference pattern appears on the glass substrate. **b)** The schematic shows the main components of the lithography setup: beam splitter (BS), mirror (M), quartz plate (QP), lens (L), photodetector (PD), and pinhole (P). **c)** The SEM image shows the triangular grating structure written with such a setup. The period and height of the grating is 1800 nm and 400 nm, respectively.

### 3. CHARACTERIZATION AND DISCUSSION

We measured the reflectance spectra of the fabricated samples in the visual regime at normal incidence ( $8^\circ$  with UV-Vis Spectrometer Lambda 1050, PerkinElmer, Massachusetts, USA). The 3-detector module was used to measure the specular reflection. Angle resolved specular reflectivity measurements were carried out with the Universal Reflectance Accessory (URA) in the range of 400–800 nm for incidence angles ranging from  $8^\circ$  to  $65^\circ$ . All measurements were recorded with unpolarized light. The measurements are done with the fully-automated variable-angle specular reflectance accessory. The quantitative optical characterization of the fabricated structures is shown in Fig. 4. As depicted in Fig. 4a), the ‘Christmas tree’ like structure has a reflection of around 30% in blue regime (380–460 nm) at normal incidence while only negligible ( $\sim 2\%$ ) reflection is observed for the triangular structure without lamellae. Consequently, it is evident that the reflectance in blue regime is caused by the six alternating layers of air and photoresist. The thickness of each layer of photoresist is approximately 40 nm and the air gap within the layers is also about 40 nm. The wavelength of the high reflection peak can be calculated from the equation describing the thin film interference.<sup>27</sup> The second order reflection at normal incidence computes to  $4(n_1d_1 + n_2d_2)$  which is 424 nm in our case ( $n_1 = 1.65$ ,  $d_1 = 40$  nm,  $n_2 = 1$ ,  $d_2 = 40$  nm). The experimentally obtained peak reflectance wavelength of 440 nm corresponds well to this theoretical value. However,

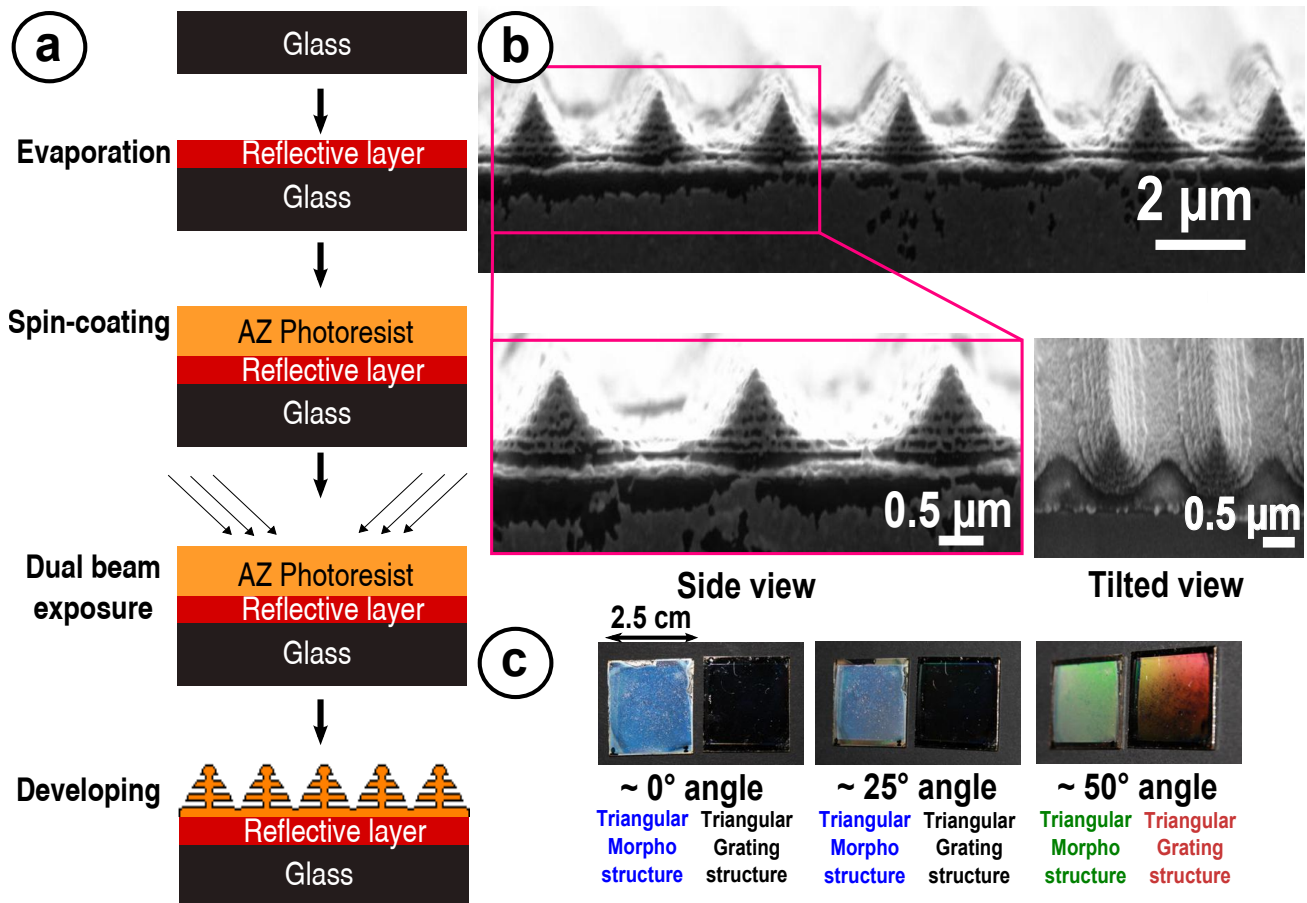


Figure 3. **a)** Flow diagram of the fabrication process of hierarchical optical structures using dual beam laser interference lithography. A reflective layer is evaporated on the clean glass substrate to obtain also a vertical structuring. After the exposure and development of the spin-coated photoresist a hierarchical structure with horizontal and vertical features appears on the substrate. **b)** An SEM image of the cross-section shows the tapered shape of the resulting ‘Christmas tree’ like structure. A closer zoom into the structure reveals the multilayers of photoresist and air within each of the ridges. **c)** Photos of the fabricated sample demonstrate the bright blue iridescence for high angles. The replicated structure is compared to the triangular grating structure (see Fig. 2) to demonstrate the different optical properties with and without vertical structuring.

the intensity of the reflection peak is low as we are only able to achieve the second order reflection due to the lower exposure wavelength. The thickness of each layer varies with the vertical period and apparently it depends mainly on the exposure wavelength and the angle of incidence (see Eq. (2)). The best exposure wavelength will be g-line (436 nm) to achieve the first order reflection. The second peak in the spectrum of the ‘Christmas tree’ like structure (Fig. 4a) at 640 nm is due to the third order reflection of the thin film interference. In addition, the lower number of layers limits the reflection intensity as well. Therefore, the reflection intensity might be improved by increasing the number of layers. The bandwidth of the reflected blue  $\Delta\lambda$  is around 122 nm. It is slightly less than the theoretical value<sup>27</sup>  $\Delta\lambda_{th} = (2/\pi)\bar{\lambda}(\Delta n/\bar{n}) \approx 130$  nm, where  $\bar{\lambda}$  is the peak-centre wavelength (424 nm),  $\Delta n$  the refractive index difference (0.65 nm), and  $\bar{n}$  the average refractive index of the air and polymer (1.325). If we consider the original Morpho butterfly using a refractive index of 1.56 for chitin<sup>2</sup> and 1 for air, the bandwidth will be 118 nm for the peak reflectance wavelength of 424 nm which is close to our experimental value. For the same reflection peak, the so far fabricated Morpho inspired multilayer replicas<sup>12,13</sup> of TiO<sub>2</sub> ( $n \approx 2.6$ ) and SiO<sub>2</sub> ( $n \approx 1.5$ ) had higher bandwidth of 145. As a lower  $\Delta n/\bar{n}$ , i.e., the bandwidth, is important for a better color impression,<sup>28</sup> the optical properties of the presented structure are better than previously reported values.<sup>12,13</sup>



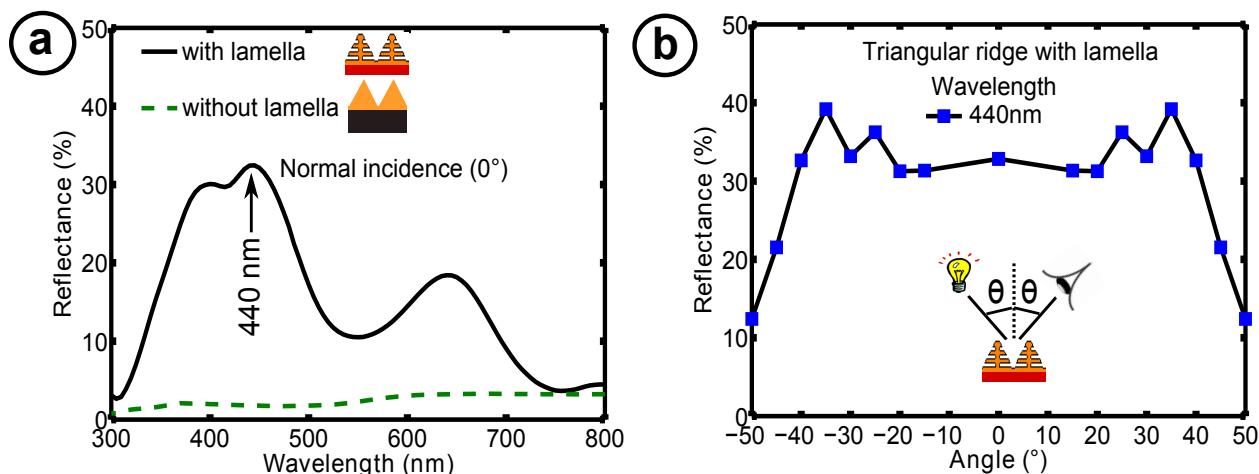


Figure 4. **a)** The reflection spectra of the two different samples are quite different. The 'Christmas tree' like sample shows a large peak in the blue regime with a reflection of about 30%. The triangular grating on the other hand has low reflection below with no specific peaks in the visible regime. **b)** The angle resolved reflection spectra of the 'Christmas tree' like sample reveals the high reflection of blue light for angles up to 40°.

The most interesting phenomena of the *Morpho* nanostructures is their omnidirectional blue non-iridescent reflection. If we consider again the classical equation of thin film interference,<sup>27</sup> the peak reflection wavelength shifts approximately by 35 nm for an incident angle of 30°. Apparently, this is not true for *Morpho* butterfly structures. As depicted in Fig. 4b), the reflection stays in the blue regime up to an angle of 40°. This effect is partly caused by the tapered shape of the multilayer air-polymer structures.<sup>11</sup> The tapered 'Christmas tree' like shape creates an impedance matching to the blue wavelength for higher angles of incidence. A rise of the reflection intensity at 440 nm occurs for an incident angle of 30° because of the horizontal periodic grating pattern. This result shows again that the 'Christmas tree' like tapered shape of lamellae is the right design to manufacture optical structures with omnidirectional non-iridescent reflection.

The *Morpho* butterfly wing features not only optically interesting phenomena but also superhydrophobicity. Its quasi hierarchical structural pattern makes it superhydrophobic and self-cleaning.<sup>14</sup> In order to examine also this feature, we performed contact angle measurements on our samples. The static contact angles were determined with the contact angle measurement system OCA 40 (DataPhysics Instruments GmbH, Filderstadt, Germany). To measure the static contact angles, water droplets with a volume of 1-4  $\mu\text{l}$  were dispensed to the surfaces (DI-water with  $\gamma_{LV} = 72 \pm 9 \text{ mNm}^{-1}$ , temperature  $\approx 22^\circ\text{C}$ , rel. humidity  $\approx 45\%$ , clean room conditions). The software SCA20 (DataPhysics Instruments GmbH, Filderstadt, Germany) was used to analyze the contact angles applying Young-Laplace fitting. The results are summarized in Fig. 5. The unstructured AZ photoresist is hydrophilic with a contact angle of 76° (Fig. 5a)). After structuring the resist, the contact angle of the triangular grating is increased to 88° but it is still below 90° (Fig. 5b)). The hierarchical 'Christmas tree' structure, however, is hydrophobic with a contact angle of 110° as depicted in Fig. 5c). The *Morpho* inspired replica, however, is not as good as the original wing surface (Fig. 5d)). This will partly be caused by the low aspect ratio of the artificial structure and the fact that chitin itself is hydrophobic.<sup>29</sup>

## 4. CONCLUSION

In summary, we successfully reproduced the *Morpho* butterfly inspired 'Christmas tree' like shape utilizing dual beam laser interference lithography. We exploit the common issue of back reflection from the substrate and specifically used it to create the vertical interference to form the lamella pattern of the *Morpho* butterfly. Our fabricated *Morpho* replica possesses the most important features of the original scale, namely the non-iridescent blue reflection till 40° and hydrophobicity. In addition to butterflies there are other insects and plants in nature that feature structural colors caused by multilayer stacks of two materials.<sup>30-32</sup> Consequently, the presented fabrication technique opens a path to manufacture these structures on large areas.

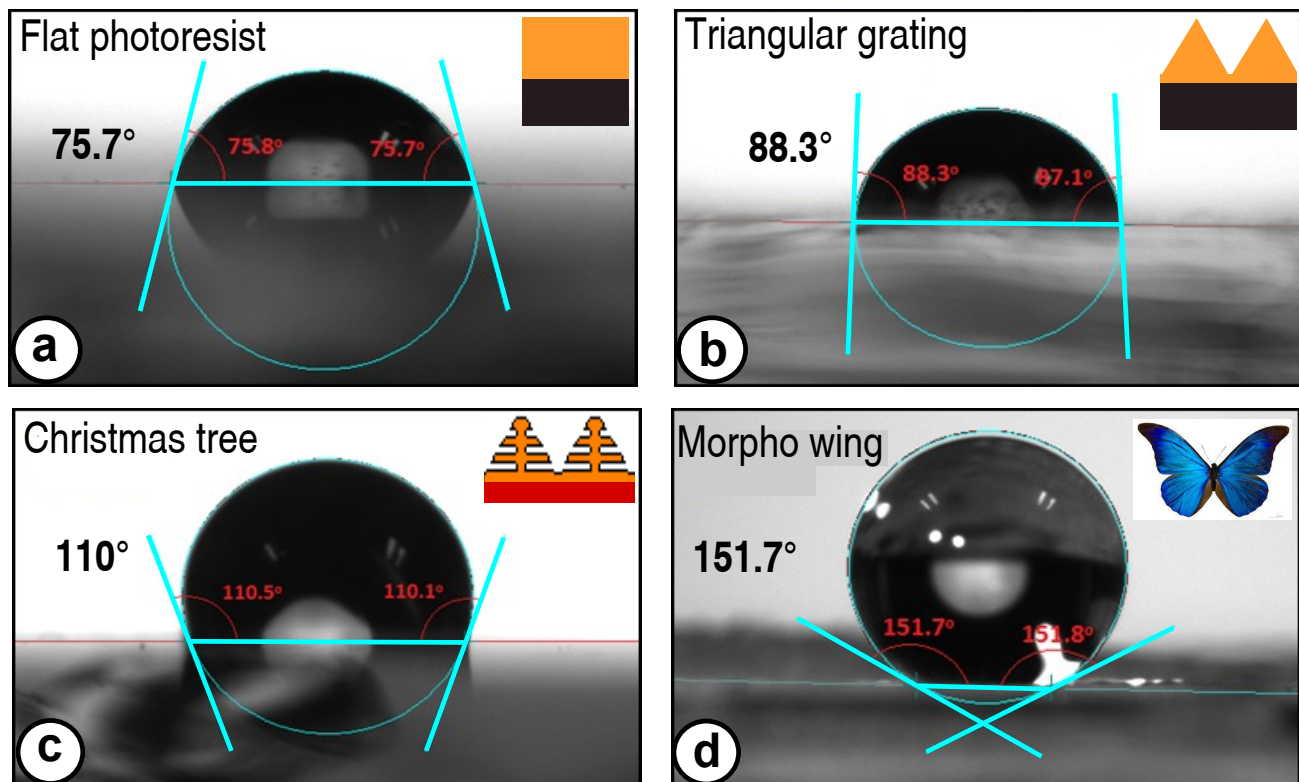


Figure 5. Comparison of the contact angles measured on the fabricated structures and an original *Morpho* wing. **a)** The flat photoresist and **b)** the one dimensional triangular grating are hydrophilic as their contact angles are less than 90°. **c)** The 'Christmas tree' like structure, however, is hydrophobic. Due to its hierarchical structuring the contact angle increased to 110°. **d)** Nonetheless, the contact angle is still lower than that of the original butterfly.

Nonetheless, there is room for improvement. An increase of the number of layers will increase the reflection intensity and the aspect ratio of the ridges at the same time. Increasing the height of the structures will improve the hydrophobicity too and might turn the surface into a superhydrophobic optical coating. As the photoresist has lower sensitivity towards exposure wavelength, it requires already higher exposure time and dosage to expose 500 nm thick resist. The lower sensitivity is necessary to obtain the tapered shape of the *Morpho* for omnidirectional blue reflection. Consequently, there is a trade off between achieving non-iridescent reflection and getting higher aspect ratio. By tuning the exposure wavelength and choosing the photoresist accordingly, structural colors with all wavelength in the visible range can be produced. Apparently, our structures can be used for several applications inspired by *Morpho* butterfly structures.

## ACKNOWLEDGMENTS

We thank Claudia Zeiger for providing the photographs of the *Morpho* butterfly. Furthermore, we acknowledge fruitful discussions with Akira Saito (Osaka University), Guillaume Gomard (KIT), and all members of the Biomimetics group at KIT. This work was partly carried out with the support of the Karlsruhe School of Optics and Photonics (KSOP, [www.ksop.idschoools.kit.edu](http://www.ksop.idschoools.kit.edu)) and the Karlsruhe Nano Micro Facility (KNMF, [www.kit.edu/knmf](http://www.kit.edu/knmf)), a Helmholtz Research Infrastructure at Karlsruhe Institute of Technology (KIT, [www.kit.edu](http://www.kit.edu)).

## REFERENCES

- [1] Ghiradella, H., "Light and color on the wing: structural colors in butterflies and moths," *Appl. Opt.* **30**, 3492 (Aug. 1991).

- [2] Vukusic, P., Sambles, J. R., Lawrence, C. R. and Wootton, R. J., "Quantified interference and diffraction in single Morpho butterfly scales," *Proc. R. Soc. B Biol. Sci.* **266**, 1403–1411 (July 1999).
- [3] Parker, A. R., "515 Million Years of Structural Colour," *J. Opt. A Pure Appl. Opt.* **2**, R15–R28 (Nov. 2000).
- [4] Kinoshita, S., Yoshioka, S., and Kawagoe, K., "Mechanisms of structural colour in the Morpho butterfly: cooperation of regularity and irregularity in an iridescent scale," *Proc. Biol. Sci.* **269**, 1417–21 (July 2002).
- [5] Gralak, B., Tayeb, G. and Enoch, S., "Morpho butterflies wings color modeled with lamellar grating theory," *Opt. Express* **9**, 567–78 (Nov. 2001).
- [6] Kinoshita, S. and Yoshioka, S., "Structural colors in nature: the role of regularity and irregularity in the structure," *Chemphyschem* **6**, 1442–59 (Aug. 2005).
- [7] Banerjee, S., Cole, J. B., and Yatagai, T., "Colour characterization of a Morpho butterfly wing-scale using a high accuracy nonstandard finite-difference time-domain method," *Micron Oxford Engl.* **1993** **38**(2), 97–103 (2007).
- [8] Zhu, D., Kinoshita, S., Cai, D., and Cole, J., "Investigation of structural colors in Morpho butterflies using the nonstandard-finite-difference time-domain method: Effects of alternately stacked shelves and ridge density," *Phys. Rev. E* **80**, 1–12 (Nov. 2009).
- [9] Smith, G. S., "Structural color of Morpho butterflies," *Am. J. Phys.* **77**(11), 1010 (2009).
- [10] Steindorfer, M. A. and Schmidt, V., "Detailed simulation of structural color generation inspired by the Morpho butterfly," *Opt. Express* **20**(19), 21485–21494 (2012).
- [11] Siddique, R. H., Diwald, S., Leuthold, J. and Hölscher, H., "Theoretical and experimental analysis of the structural pattern responsible for the iridescence of Morpho butterflies," *Opt. Exp.* **21**, 14351 (June 2013).
- [12] Saito, A., Murase, J., Yonezawa, M., Watanabe, H., Shibuya, T., Sasaki, M., Ninomiya, T., Noguchi, S., Akai-kasaya, M., and Kuwahara, Y., "High-throughput reproduction of the Morpho butterfly's specific high contrast blue," *Proc. SPIE* **8339**, 83390C–83390C–10 (2012).
- [13] Chung, K., Yu, S., Heo, C., Shim, J. W., Yang, S., Han, M. G., Lee, H., Jin, Y., Lee, S. Y., Park, N. and Shin, J. H., "Flexible , Angle-Independent , Structural Color Re flectors Inspired by Morpho Butterfly Wings," *Adv. Mater.* **24**, 2375–2379 (May 2012).
- [14] Zheng, Y., Gao, X. and Jiang, L., "Directional adhesion of superhydrophobic butterfly wings," *Soft Matter* **3**(2), 178 (2007).
- [15] Potyrailo, R. A., Ghiradella, H., Vertiatchikh, A., Dovidenko, K., Cournoyer, J. R. and Olson, E., "Morpho butterfly wing scales demonstrate highly selective vapour response," *Nat. Photonics* **1**(2), 123–128 (2007).
- [16] Pris, A. D., Utturkar, Y., Surman, C., Morris, W. G., Vert, A., Zalyubovskiy, S., Deng, T., Ghiradella, H. T., and Potyrailo, R. A., "Towards high-speed imaging of infrared photons with bio-inspired nanoarchitectures," *Nat. Photonics* **6**, 195–200 (2012).
- [17] Zhang, W., Zhang, D., Fan, T., Gu, J., Ding, J., and Wang, H., "Novel Photoanode Structure Templated from Butterfly Wing Scales," *Chem. Mater.* **21**(1)(3), 33–40 (2009).
- [18] Aryal, M., Ko, D., Tumbleston, J. R., Gadisa, A., Samulski, E. T., and Lopez, R., "Large area nanofabrication of butterfly wing ' s three dimensional ultrastructures Large area nanofabrication of butterfly wings three dimensional ultrastructures," *J. Vac. Sci. Technol. B* **30**, 061802 (2012).
- [19] Campbell, M., Sharp, D., Harrison, M. T., Denning, R. G., and Turberfield, A. J., "Fabrication of photonic crystals for the visible spectrum by holographic lithography," *Nature* **404**, 53–6 (Mar. 2000).
- [20] S. R. J. Brueck, "Optical and interferometric lithography – nanotechnology enablers," *Proc. IEEE* **93**, 1704–1720 (2005).
- [21] Jang, J.-H., Ullal, C.K., Maldovan, M., Gorishnyy, T., Kooi, S., Koh, C. and Thomas, E.L., "3D Micro- and Nanostructures via Interference Lithography," *Adv. Funct. Mater.* **17**, 3027–3041 (Nov. 2007).
- [22] Maldovan, Martin and Thomas, Edwin L, [*Periodic Materials and Interference Lithography: For Photonics, Phononics and Mechanics*], John Wiley & Sons (2009).
- [23] Wolferen, H., and Abelman, L., "Laser interference lithography," (2011).
- [24] Xie Q., Hong M.H., Tan H.L., Chen G.X., Shi L.P. and Chong T.C., "Fabrication of nanostructures with laser interference lithography," *Journal of Alloys and Compounds* **449**(12), 261 – 264 (2008).
- [25] Efremow, N. N., "A simple technique for modifying the profile of resist exposed by holographic lithography," *J. Vac. Sci. Technol.* **19**, 1234 (Nov. 1981).



- [26] MicroChemicals GmbH<sup>®</sup>, “Az<sup>®</sup> 1500-series.”
- [27] Kolle, M., Salgard-Cunha, P. M., Scherer, M. R. J., Huang, F., Vukusic, P., Mahajan, S., Baumberg, J. J. and Steiner, U., “Mimicking the colourful wing scale structure of the *Papilio blumei* butterfly,” *Nat. Nanotechnol.* **5**(7), 511–5 (2010).
- [28] Chung, K. and Shin, J. H., “Range and stability of structural colors generated by Morpho-inspired color reflectors,” *J. Opt. Soc. Am. A. Opt. Image Sci. Vis.* **30**, 962–8 (May 2013).
- [29] Kumar, M.N.V.R., “A review of chitin and chitosan applications,” *Reactive and Functional Polymers* **46**(1), 1 – 27 (2000).
- [30] Vukusic, P., Sambles, J. R. and Lawrence, C. R., “Colour mixing in wing scales of a butterfly,” *Nature* **404**, 457 (Mar. 2000).
- [31] Seago, A. E., Brady, P., Vigneron, J., and Schultz, T. D., “Gold bugs and beyond: a review of iridescence and structural colour mechanisms in beetles (Coleoptera),” *J. R. Soc. Interface* **6**, S165–84 (Apr. 2009).
- [32] Vignolini, S., Moyroud, E., Glover, B. J., and Steiner, U., “Analysing photonic structures in plants,” *J. R. Soc. Interface* **10**, 20130394 (Oct. 2013).